SARCOMERIC DOMAIN ORGANIZATION WITHIN SINGLE SKINNED RABBIT PSOAS FIBERS AND ITS EFFECTS ON LASER LIGHT DIFFRACTION PATTERNS

BERNHARD BRENNER
Institute of Physiology II, University of Tübingen, D-7400 Tübingen, Federal Republic of Germany

ABSTRACT Total intensity and fine structure of first-order laser light diffraction maxima from single skinned rabbit psoas fibers were studied. Total intensity of the diffraction maxima was measured as a function of the incidence angle (ω-scan). In the most homogenous fibers, most of the intensity in the diffraction maxima is confined to a rather narrow range of incidence angles. Fibers with less homogenous striation patterns, apparently composed of several regions of distinct sarcomere length and tilt of striation (domains), give rise to several narrow intensity peaks in their ω-scans. Left and right first-order diffraction lines produce ω-scans of almost identical shape, composed of one or more intensity peaks, with each pair of corresponding peaks separated by about the same angle. The data indicated that in single skinned rabbit psoas fibers, light diffraction is dominated by Bragg diffraction and that the peaks within ω-scans can be directly correlated with domains within the illuminated fiber segment. In the most homogenous fiber segments the diameter of domains, estimated from the width of the corresponding maxima in the ω-scans, could almost be as large as the fiber diameter. On average, from the number of peaks in the ω-scans two to three domains with an average length of ~250–350 μm can be identified in a fiber cross-section. Therefore, on average only a small number of domains (8 per mm) are found within skinned rabbit psoas fiber segments.

In contrast, the number of substructural lines within the diffraction maxima is large even for microscopically homogenous fibers. Substructural lines appear to be present only when several domains are illuminated simultaneously. Separation and width of these substructural lines are approximately inversely proportional to the length of the illuminated region of the fiber. These data suggest that the substructural lines are due to interference between domains, illuminated simultaneously by a light source with a high degree of spatial coherence (laser). The relevance of these findings for measurements of sarcomere length by laser light diffraction is discussed.

INTRODUCTION

In recent years, laser light diffraction has been widely used to measure sarcomere lengths of striated muscle preparations because their rather regular cross-striation gives rise to well-defined diffraction patterns. Typical diffraction patterns consist of a series of line-shaped diffraction maxima with strong first orders but much weaker higher orders. In addition, within each intensity maximum there are many discrete substructural lines, first described by Cleworth and Edman (1972). For sarcomere length measurements, it is usually assumed that muscle-fiber preparations represent homogenous gratings. Therefore, the position of the first-order diffraction maximum is thought to yield a sarcomere length representative of the whole region of the preparation illuminated by the laser beam. However, light micrographs of single, intact (Huxley, 1974) or skinned frog fibers (Moss, 1979) and of single skinned rabbit psoas fibers (Brenner, 1983) show that these fibers are not homogenous at all, but are organized into domains, i.e., regions distinguished by a characteristic sarcomere length and tilt of striation, both of which can vary significantly from domain to domain. If light diffraction by muscle fibers can be described as Bragg diffraction (Rüdel and Zite-Ferenczy, 1979*a*), only those domains that fulfill the Bragg condition will contribute to the diffraction pattern. Therefore, at a certain incidence angle usually only some of the domains will contribute to the diffraction pattern. Hence, the sarcomere length derived from the position of the first-order diffraction maximum is not necessarily representative of all the domains within the illiminated area of the fiber. This domain structure could lead to apparent discontinuities in the sarcomere length signal when experimental maneuvers cause changes in sarcomere length and/or striation tilt, thereby enabling different domains with different average sarcomere length to dominate the diffraction pattern. Consequently, to measure sarcomere length with high accuracy by laser light diffraction, the signal has to be sampled either from a single domain or from the same group of domains throughout an experiment. In either case, a reliable approach is required to identify and monitor individual domains and their arrangement within the illuminated fiber region.

The effects of the sarcomeric domain organization on the laser light diffraction pattern might have the potential

to identify and monitor individual domains within fiber segments. As mentioned earlier, interpreting light diffraction from muscle fibers as Bragg diffraction (Rüdel and Zite-Ferenczy, 1979*a*, *b*), a single domain will produce a line-shaped first-order diffraction maximum only when the incidence angle of the laser beam (ω) satisfies the Bragg condition. Thus, a high intensity in the first-order diffraction maximum of such a domain will be confined to a narrow range of incidence angles, producing a narrow peak when intensity is measured as a function of the incidence angle ω of the laser beam (ω-scan). On this basis, Rüdel and Zite-Ferenczy (1979*a*, *b*) postulated that each of the peaks they observed in ω-scans of frog fibers represented the contribution of a single domain. Furthermore, these authors postulated (1979*b*) that each substructural line within the diffraction maxima of a muscle fiber represented the line-shaped diffraction maximum of a single domain. Since frog fibers apparently are composed of many domains of different sarcomere length and tilt of striation, at any incidence angle the Bragg condition could be met or almost met by several domains. That is, at any incidence angle several domains could contribute to the diffraction maximum of the fiber. Thus, the broad ω-scans (see Fig. 3 in Rüdel and Zite-Ferenczy, 1979*a*; and Fig. 1 in 1979*b*) were believed to be composed of many overlapping peaks of intensity, and the numerous substructural lines observed at any incidence angle appeared to be explained. On the basis of this interpretation, in principle ω-scans and the substructural lines within the diffraction maxima appeared suitable to identify and monitor individual domains within an illuminated fiber area. However, because of the complexity of ω-scans observed in frog fibers and because of possible additional peaks in the ω-scans due to thick grating effects (Baskin et al., 1981), ω-scans appeared unsuitable for monitoring individual domains and their arrangement within fiber segments. Instead, attempts were made to directly correlate the substructural lines within the diffraction maxima with single domains within the illuminated fiber region (Tameyasu et al., 1982; Leung, 1983; Zite-Ferenczy et al., 1984; Sundell et al., 1984, 1985) and to use the position of the substructural lines to calculate the sarcomere length of individual domains (Tameyasu et al., 1982; Leung, 1983).

In skinned rabbit psoas fibers, however, it is found that although light micrographs show much more regularity of the striation pattern than frog fibers, the diffraction maxima are still composed of a large number of substructural lines, while the number of narrow peaks in the ω-scans appeared to be about the same as the number of domains identified by light microscopy. This observation is inconsistent with the interpretation of Rüdel and Zite-Ferenczy (1979*b*), Tameyasu et al. (1982), Leung (1983), Zite-Ferenczy et al. (1984), and Sundell et al. (1984, 1985).

To obtain a reliable method for gathering information about the sarcomeric domain organization within an illuminated area of rabbit psoas fibers, I reinvestigated the effects of the sarcomeric domain organization on total intensity of the diffraction maxima (ω-scans) and the origin of the substructural lines. In this study, I found that in skinned rabbit psoas fibers light diffraction is dominated by Bragg diffraction. Furthermore the validity of a direct correlation between maxima in ω-scans and domains in the fiber segment was established. Finally, the substructural lines in the diffraction maxima were found to be the result of interference between different domains and, so, do not reflect diffraction maxima of single domains. Therefore, ω-scans, but not the substructural lines, can be used to characterize the sarcomeric domain organization in single skinned rabbit psoas fibers. The implications of these results in measuring sarcomere length with high accuracy are discussed.

Preliminary account of this work has been reported briefly (Brenner, 1985).

METHODS

Fiber Preparation

Single skinned rabbit psoas fibers were dissected and mounted according to Brenner (1980, 1983). Care was taken to remove all surrounding material from the fiber surface to avoid artifacts in the laser diffraction pattern.

Solutions

Table I shows the composition of solutions. Fibers were stored up to 3 d in skinning solution in the refrigerator (~5°C). A few experiments were also performed with fibers stored for up to 1 wk in 1:1 (vol/vol) glycerol:skinning solution at −20°C. All experiments were done in relaxing solution at 5°C and pH 7.0 with the ionic strength adjusted to 170 mM by adding the appropriate amount of KCl.

Laser Diffraction System

A schematic drawing of the laser diffraction system is shown in Fig. 1. To vary the incidence angle of the laser beam, the fiber could be rotated within the trough around an axis perpendicular to fiber and laser beam. This way, the geometry of the optical system was not altered when the incidence angle was changed. To ensure that always the same area of the fiber was illuminated, I placed the axis of rotation in the center of the

TABLE I
COMPOSITION OF SOLUTIONS

	Imidazole	KH_2PO_4	Mg-Acetate	$MgCl_2$	ATP	EGTA	K-Propionate	KCl
Skinning solution	—	5*	3	—	3–6	5	75	—
Relaxing solution	10	—	—	3	1	1	—	150

*All in mM. All solutions adjusted to pH 7.0 at 5°C.

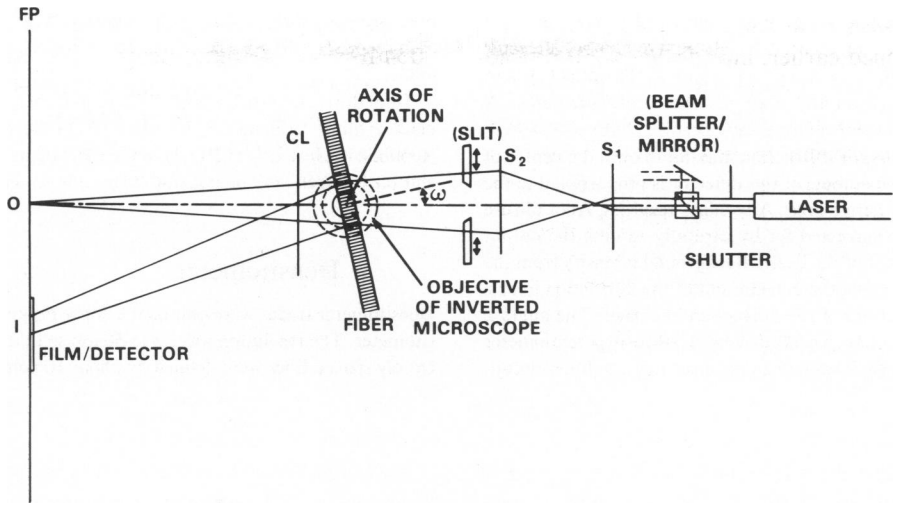

FIGURE 1 Schematic drawing of the diffraction system (viewed from the top). S_1 and S_2 are microscope eyepieces, arranged to collimate or expand the original laser beam. *FP* is the focal plane of the S_1-S_2 combination. Light detector and film were placed in this plane. *CL* is a combination of cylindrical lenses with a numerical aperture (NA) of 0.78 (λ = 632.8 nm) that was used to vertically focus the diffraction lines onto the light detector. The combination of beam-splitter and mirror was used for the double-beam experiments. The slit in front of the fiber, in combination with beam expansion, was used as an alternative way to vary the length of the illuminated fiber area. ω is the angle between laser beam and normal on fiber axis. The axis of fiber rotation intersects the fiber at the center of the illuminated area.

fiber area illuminated by the laser beam. This adjustment was controlled by an inverted microscope.

Combinations of microscope oculars (Leitz periplan GF 10× or Huygens 6×), placed between laser source and fiber, were used to focus the original, collimated, or expanded laser beam onto the plane where the diffraction pattern was to be studied. In some control experiments the oculars were placed such that the expanded or collimated laser beam were parallel. The diameter of the illuminated fiber area was varied in two ways: either the beam was expanded by proper selection of the ocular combination and the length of the illuminated fiber section was defined by a set of slits right in front of the fiber; or the size of the illuminated area was varied by using different combinations of oculars.

For double-beam illumination, a combination of a cubic beam splitter and a mirror were placed between laser source and oculars. The separation of the beams could be varied by moving the mirror relative to the beam splitter. The orientation of the beams, adjustable by rotating the mirror, was choosen to ensure that the focal points of the two beams were superimposed in the focal plane. Separation and size of the illuminated areas could be estimated using the inverted light microscope.

To measure total intensity within the first-order diffraction line as a

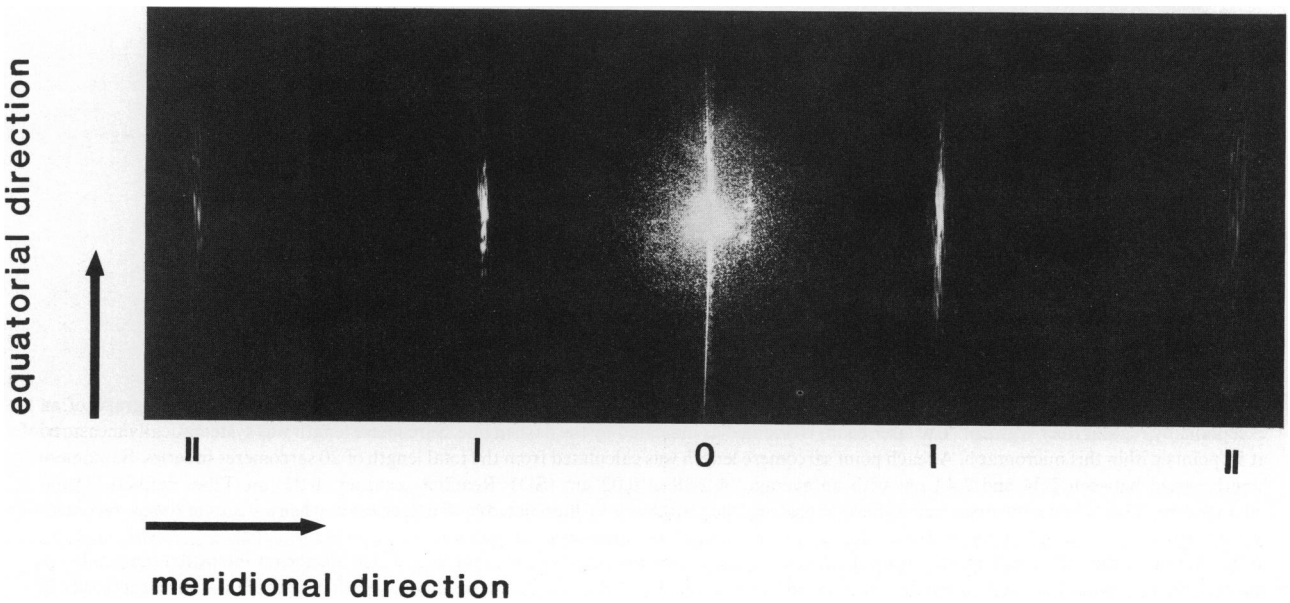

FIGURE 2 Typical laser diffraction pattern of a single skinned rabbit psoas fiber at perpendicular beam incidence (ω = 0). To enhance the second orders on the film, the areas around the second orders were exposed about three times as long as the center of the pattern. Fiber-film distance, 70 mm; sarcomere length measured by the light microscope is 2.3 μm.

function of the incidence angle ω (for the definition of ω, see Fig. 1), I placed a position-sensitive detector (PIN SC-10/D; United Detector Technology, Santa Monica, CA) in the focal plane of the optical system that was set to 100 mm from the fiber for these measurements. A cylindrical lens combination with a numerical aperture (NA) of 0.78 (λ = 632.8 nm) was used to focus the diffraction maximum onto the center of the detector. The sum of the outputs of this detector is proportional to the total light intensity on the active area. Any offset resulting from diffuse background light could be corrected for by carefully zeroing the output when the fiber was moved out of the beam. Background intensity from the fiber itself, estimated by moving the detector out of the diffraction line, is <1% of the maximum intensity of the diffraction line itself. The angle ω was monitored using a friction wheel, driving a 10-turn potentiometer that was used as the feed-back resistor in an inverting amplifier circuit. Both signals, angle ω and total intensity, were displayed on a storage oscilloscope (5103N; Tectronix, Inc., Beaverton, OR) using the *x-y* mode.

Total diffraction patterns or diffraction maxima were photographed by placing film (Agfapan 25, 3 × 4 in [Agfa Gevaert, Munchen, Federal Republic of Germany (FRG)]) in the focal plane of the optical system. A shutter between laser source and fiber allowed timing of the exposure.

Densitometer

Densitometer traces were obtained using a Perkin Elmer PDS microdensitometer. The resolution was set to 50 μm so that the narrowest and most closely spaced lines were defined by about 10 points (peak to peak).

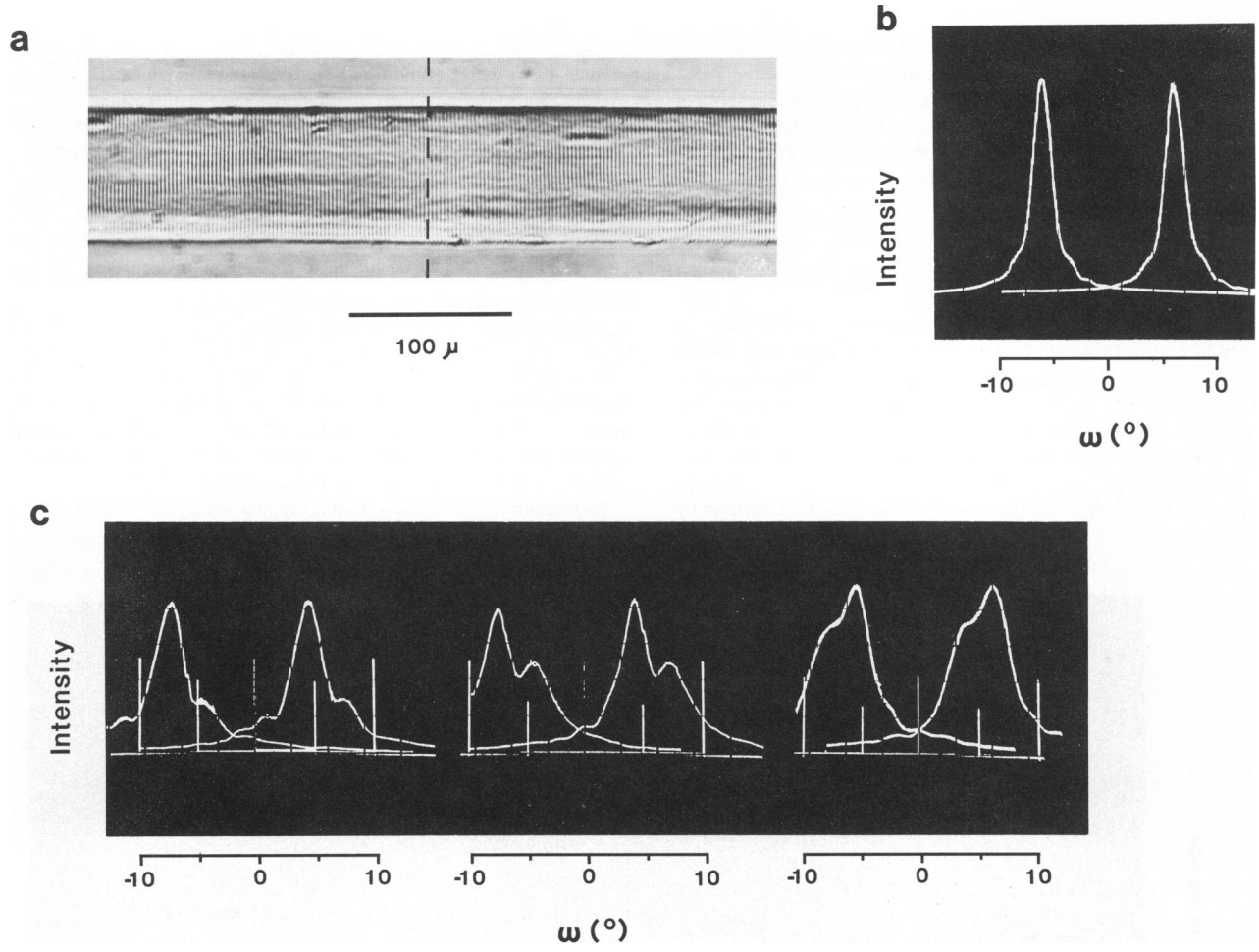

FIGURE 3 Effect of beam incidence angle ω on the total intensity of the first order diffraction maximum (ω-scan). (*a*) Micrograph of an exceptionally regular fiber segment. The laser beam is oriented as indicated by the dashed line. Sarcomere length was systematically measured at 70 points within this micrograph. At each point sarcomere length was calculated from the total length of 20 sarcomeres in series. Sarcomere length varied between 2.34 and 2.42 μm with an average of 2.38 ± 0.02 μm (SD). Reading accuracy, 0.01 μm. Fiber diameter (from micrograph), 85 μm. Note, the fiber region shown represents the area that was illuminated by the laser beam when ω-scans of *b* were recorded. (*b*) ω-scans of left- and right-hand first-order diffraction maxima of the same fiber segment shown in *a*. Abscissa, angle ω; ordinate, intensity in the first-order diffraction maximum. Beam diameter, 0.5 mm. Note the very narrow range over which significant intensity is detectable in the first orders. This is found only when the striation pattern is as regular as it is in *a*. At perpendicular beam incidence (ω = 0), the intensity in either first-order maximum is only about 1/20 of the maximum observed when the incidence angle is about ±6°. (*c*) Three typical ω-scans of single skinned rabbit psoas fibers with somewhat less regular striation patterns. Coordinates same as in *b*. Note the almost identical shape and amplitude of the two ω-scans in all cases. Each pair appears to be composed of almost identical maxima separated by about the same angle. To demonstrate the high reproducibility of these ω-scans, all records were traced several times (traces superimposed).

Light Microscopy

Sarcomere length and striation tilt were measured from light micrographs taken with an inverted microscope (Leitz Ortholux II, modified for use as an inverted microscope; film: Agfaortho 25 [Agfa Gevaert] or Kodak Technical Pan Film 2415 [Eastman Kodak Co, Rochester, NY]). The optical axis of the inverted microscope was parallel to the axis of rotation for the ω scans. The microscope was also used to monitor continuously fiber integrity and to estimate length of the illuminated area of the fiber and the separation of the illuminated areas in double-beam experiments. In addition, the microscope was needed for adjustment and monitoring of the axis of rotation for the ω-scans to ensure that during such a scan the same fiber area stayed illuminated.

RESULTS

Laser Light Diffraction Patterns of Single Skinned Rabbit Psoas Fibers

A typical diffraction pattern of a single skinned rabbit psoas fiber at normal beam incidence is shown in Fig. 2. In contrast to diffraction patterns from whole frog muscle (Sandow, 1936; Cleworth and Edman, 1972) or single frog fibers (Cleworth and Edman, 1972; Zite-Ferenczy and Rüdel, 1978), only the two first-order maxima, besides the zero order, are prominent. Second or higher orders are very faint or invisible. To demonstrate the presence of second order diffraction maxima in Fig. 2, I had to expose the areas around the second orders about three times as long as the inner part of the diffraction pattern. Only from fibers with less regular striations were second or higher orders directly detectable at normal beam incidence.

Total Intensity within First-order Diffraction Maxima at Various Incidence Angles (ω-Scans)

The effect of the beam incidence angle on the total intensity of the first-order diffraction maximum (ω-scans) is shown in Fig. 3. In fibers with an exceptionally regular striation pattern (Fig. 3 *a*), a significant total intensity in the first-order diffraction maximum is observed within a very narrow range, for example, 2.2° full width at half maximum intensity (FWHM) in Fig. 3 *b*. This shows that at normal beam incidence even the intensity within the first-order line is far from the maximum and is more than 20-fold enhanced when the beam incidence angle is varied to maximize intensity in one of the first orders: to about ±6° from normal beam incidence for the left and right first order. Since the maxima for total intensity of the second-order diffraction lines are located around ±12° (not shown in Fig. 3 *b*), these orders are hardly visible at perpendicular beam incidence. In ω-scans of less homogenous fibers, more than one peak for total intensity of the diffraction lines can be observed (Fig. 3 *c*).

Comparison of ω-scans from both left- and right-hand first-order diffraction lines (Fig. 3, *b* and *c*) shows that the overall shape of the two ω-scans is very similar. Each pair of ω-scans, if composed of several peaks, appears almost identical in shape and size, and corresponding peaks are separated by approximately the same angle. This was found in all 12 experiments in which both ω-scans, i.e., for left and right first order, were recorded. In no case could intensity peaks be found that did not fulfill these criteria. In particular, no pair of ω-scans was found with the corresponding intensity peaks located around a symmetry plane, as was postulated for peaks due to grating diffraction (see Figs. 7 and 8 in Baskin et al., 1981).

Correlation of Intensity Peaks in ω-Scans with Domains in Light Micrographs

To test whether each peak of total intensity in the ω-scans might represent the contribution of one single domain within the illuminated fiber segment, I measured sarcomere length and striation tilt from micrographs of illuminated fiber segments. These two parameters were then used to calculate the necessary beam incidence angles to observe intensity peaks in the first-order diffraction lines, i.e., the incidence angle necessary to fulfill the Bragg condition (for calculation of angle ω, see first part of Appendix). Comparison of the calculated incidence angles with the experimentally measured angles at which intensity peaks were actually observed (Fig. 4) shows a rather close correlation. For accurate measurements of sarcomere length and striation tilt and for less ambiguous correlation between calculated and measured incidence angles, I rejected fiber segments that produced more than three distinct and prominent peaks in the ω-scans. Also, areas were sought with pronounced tilt of striation to test the postulated correlation over a wide range of angles.

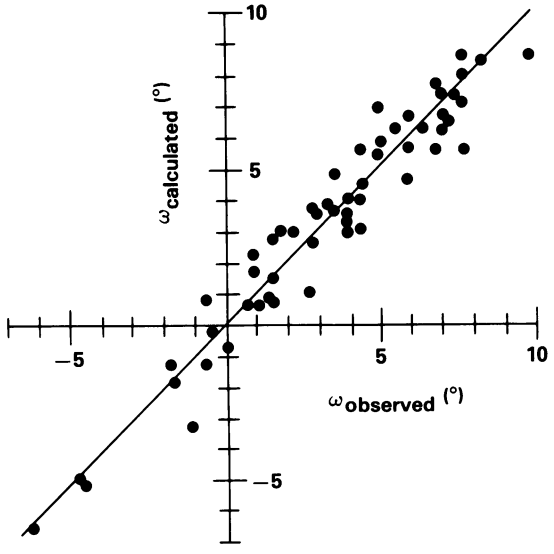

FIGURE 4 Necessary incidence angle ω to observe maximum intensity in ω-scans calculated from sarcomere length and straition tilt ($\omega_{calculated}$) vs. angle ω, at which maximum intensity is observed in the ω-scan of the same fiber area ($\omega_{observed}$). Sarcomere length and striation tilt were measured from micrographs of the illuminated fiber area. The necessary incidence angle ω to observe maximum intensity in ω-scans was calculated from the Bragg equation. For details see first part of the Appendix. Data of eight different fibers are summarized.

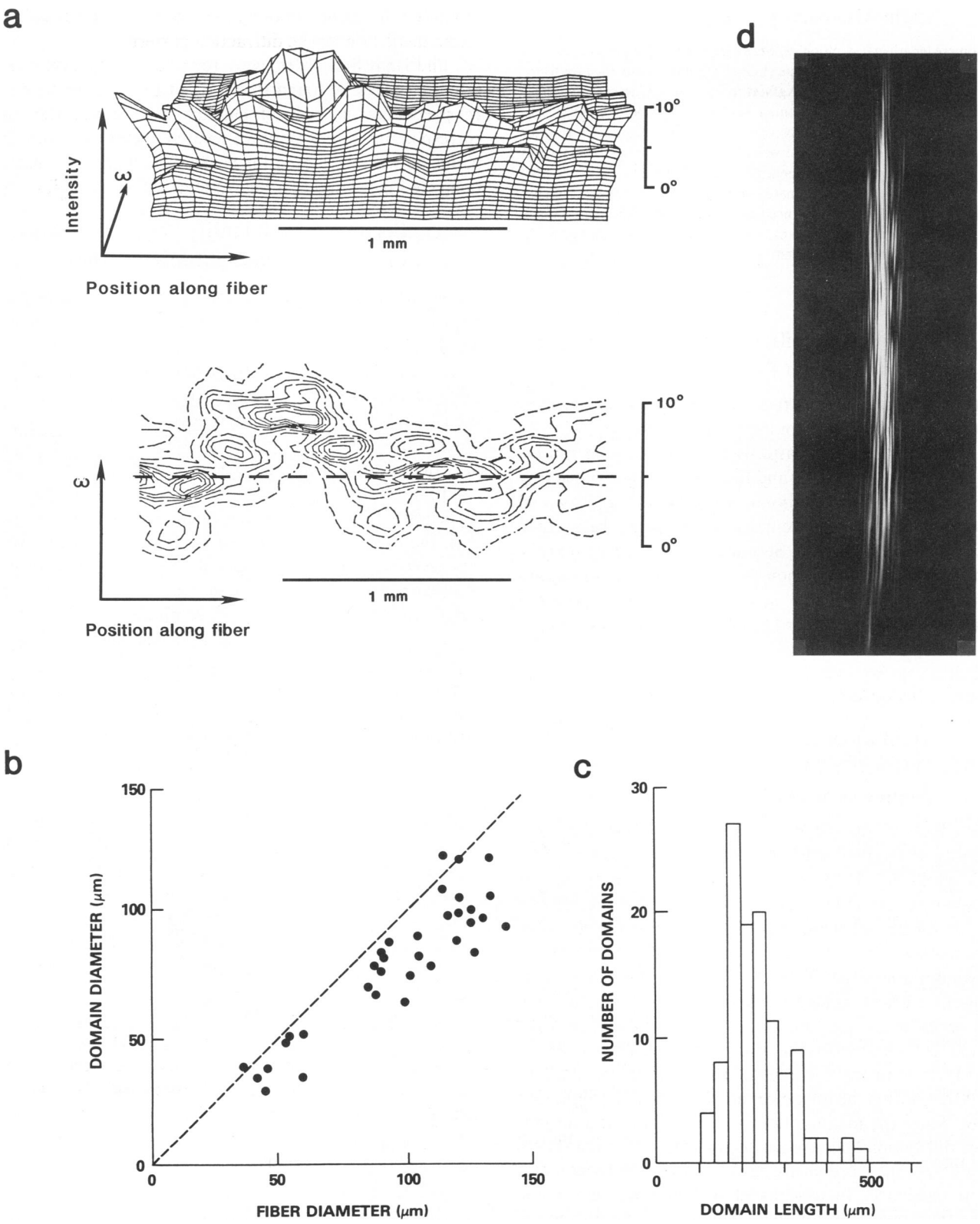

FIGURE 5 Size and number of domains within a fiber segment, determined from ω-scans, vs. substructural lines within the first-order diffraction line. (*a*) Display of a series of ω-scans along a fiber segment as a three-dimensional map (top) and as a corresponding intensity contour map (bottom). ω-scans were recorded every 60 μm. Total segment length represented by this series is ~2 mm. Beam diameter ~60 μm. Note the length along the fiber and the narrow range of incidence angles for which a single peak of intensity can be followed. Taking each individual peak as the contribution of a single domain, about 15 domains can be identified. At the incidence angle, which is indicated by the dashed line in the contour map, at most five domains will contribute to the diffraction pattern of the 2-mm segment. (*b*) Diameter of domains estimated from the FWHM of the intensity peaks in ω-scans vs. fiber diameter. For details of calculation see second part of the Appendix. The

Size of Domains Determined by Series of ω-Scans

Since a close correlation is found between intensity peaks in ω-scans and single domains within the illuminated fiber segment (Fig. 4), ω-scans measured at various positions along a fiber were used to define the sarcomeric domain organization of fibers. Estimating the diameter of the diffracting units (domains) from the FWHM of the intensity peaks in the ω-scans (Fig. 5, *a* and *b;* for calculation, see second part of Appendix) shows that the diameter of the largest domains can be as large as the fiber diameter, i.e., up to 120–150 μm. By following domains along fibers, as shown by the appearance and disappearance of intensity peaks in a series of ω-scans (Fig. 5 *a*), one sees that the average length of domains is ~200–250 μm, and sometimes as long as 600–700 μm (Fig. 5 *c*). The number of domains within a cross-section of the fiber segments, counted from the number of peaks within the ω-scans, varied between one and three major domains (Fig. 3, *b* and *c* and Fig. 5 *a*). By also counting rather small intensity peaks in the ω-scans, which possibly originated from very small domains, sometimes up to five or six domains could be identified in a cross-section. Thus, from the intensity peaks in ω-scans, only a small number of domains, about 15, can be identified within a 2-mm fiber segment (Fig. 5 *a*).

Results Inconsistent with a Direct Correlation between Substructural Lines and Single Domains

If each substructual line and each intensity peak within the ω-scans represents the contribution of one single domain to the diffraction line of a fiber segment (Rüdel and Zite-Ferenczy, 1979*b*), then at each incidence angle the number of substructural lines within the diffraction maximum and the number of peaks in the ω-scans contributing to the diffraction line should be the same, both reflecting the number of domains contributing to the diffraction maximum at this incidence angle. However, in Fig. 5 *a* we have shown that in the 2-mm fiber segment only a small number of domains contribute to the diffraction line at any one incidence angle. This is in contrast to the large number of substructural lines observed for all incidence angles (see Fig. 5 *d* as example for incidence angle of 5°). This observation is inconsistent with the idea that both individual intensity peaks in ω-scans and individual substructural lines within the diffraction lines reflect the contribution of a single domain to the diffraction pattern.

The hypothesis that each substructural line represents the diffraction maximum of one domain also predicts that these substructural lines should be unaffected whether domains are illuminated one by one or all at once. This prediction was tested by recording the diffraction pattern of a fiber segment by, first, illuminating an area of ~4-mm length simultaneously (Fig. 6 *b*) and, second, by illuminating sequential fractions of this area, 0.3–0.5 mm in length, by means of a slit in front of the fiber. The diffraction maxima of all of these fractions were added up by repeated exposure of the film used to record the diffraction maxima (Fig. 6 *a*). The slit width was chosen between 0.3 and 0.5 mm, since this was slightly larger than the average length of domains when determined by a series of ω-scans (Fig. 5). Surprisingly, the substructural lines observed in Fig. 6 *b* are virtually absent in Fig. 6 *a*, in apparent contradiction with the prediction from a direct correlation between substructural lines and single domains.

Again, assuming that a substructural line represents the diffraction maximum of a single domain, one can calculate the necessary length of a domain to produce the observed width of the substructural lines. In Fig. 7 *a,* part of a diffraction maximum of a fiber is shown, together with a typical densitometer trace across this diffraction maximum. From this densitometer trace the average width of substructural lines can be estimated (0.32 ± 0.01 mm). The relation between domain length and angular width of the resulting diffraction maximum is $\Delta\theta = \lambda/(l \cos\theta)$, where θ is polar angle between the zero and the first order, l is the length of the domain, and λ is the wave-length of HeNe laser (Guinier, 1963). From this equation, at a sarcomere length of 2.4–2.5 μm the calculated domain length, necessary to produce the observed average line width of 0.32 mm, is ~3.6 mm. In this calculation, no variation in sarcomere length within the domains is assumed. Thus, the required domain length is at least about equal to the length of the illuminated area. Therefore, by reducing this length, i.e., by reducing the illuminated part of the assumed domains, all of the narrow substructural lines should simply become wider. However, experimentally both line width and separation of the substructural lines were found to increase when the beam diameter was reduced (Fig. 7, *b, c,* and *d*), while the number of substructural lines decreased approximately proportionally with the beam diameter. These findings again are in disagreement with the prediction from the

abscissa is the fiber diameter and the ordinate is the calculated domain diameter, both measured in micrometers. Beam diameter, ~60 μm. Note that the diameter of the domains is about proportional to the fiber diameter and can almost reach the fiber diameter (dashed line). (*c*) Histogram of domain length, estimated from the length along the fiber for which a domain could be followed as a distinct peak in a series of ω-scans. Abscissa, length of domains in micrometers; ordinate, number of domains. Note, that on average domains can be followed over ~200–250 μm. (*d*) First-order diffraction maximum observed at the incidence angle indicated by a dashed line in the contour map (*a*). Note that the number of substructural lines is much larger than five, which is the number of peaks in the ω-scans found to contribute to the diffraction maximum at this incidence angle (*a*). Fiber-film distance, 315 mm; beam diameter, 2 mm.

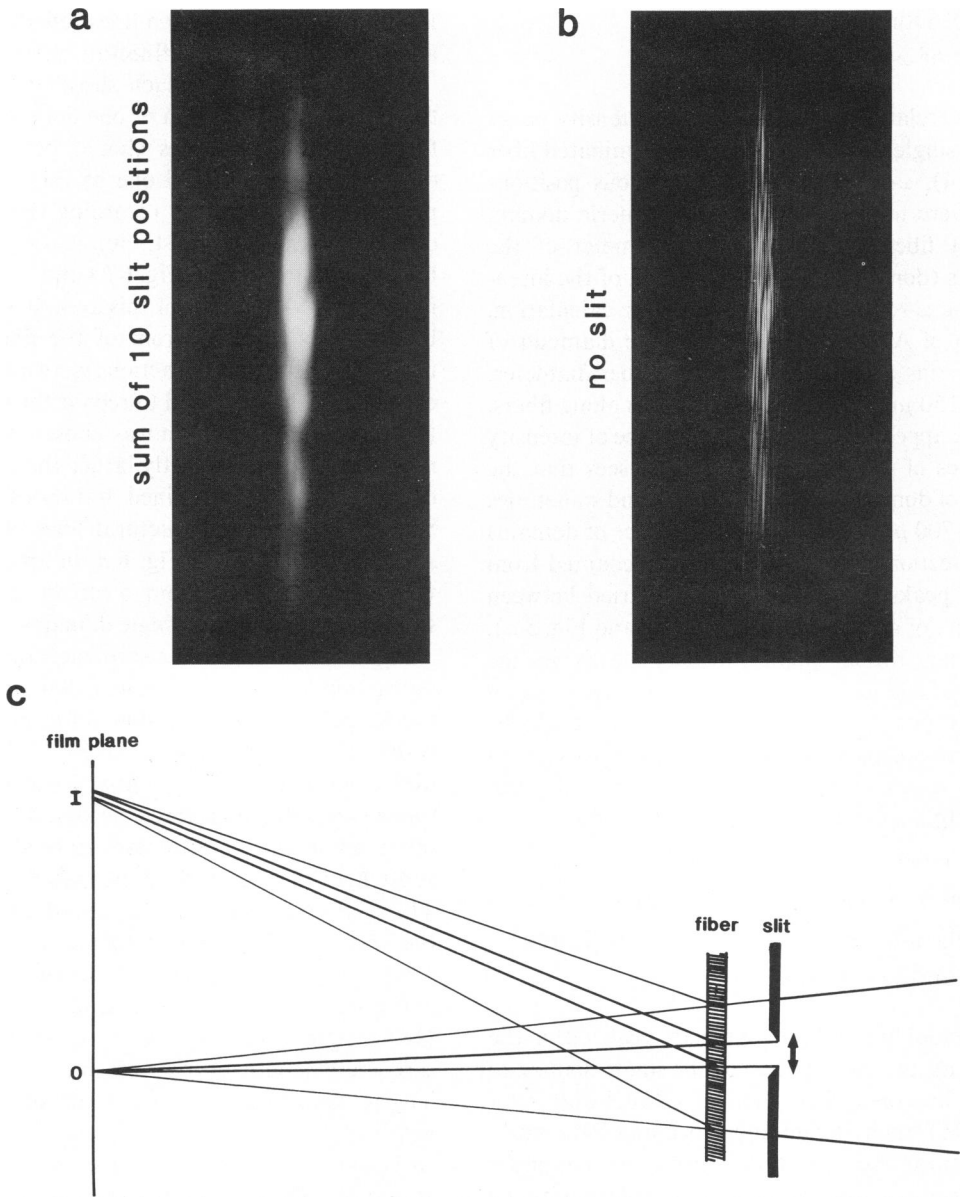

FIGURE 6 Effect of simultaneous and successive illumination of a fiber segment. (*a*) Fiber segment illuminated successively, section by section, by means of the slit in front of the fiber. Width of slit, 0.45 mm. All resulting first-order diffraction maxima were recorded on the same film (multiple exposure). (*b*) Fiber segment illuminated without slit, using the total expanded beam. Beam diameter, 3.8 mm. Fiber-film distance, 400 mm. (*c*) Schematic drawing of the optical arrangement. Beam expanded and focused onto the film plane by two eyepieces, S_1 and S_2 (see Fig. 1). This arrangement insures that the intensity distribution, and, thus, the relative illumination of each section along the fiber, is similar for both simultaneous and successive illumination.

hypothesis that each substructural line represents the diffraction line of a single domain.

Evidence for Interference between Different Fiber Areas

Since diffraction maxima are different when a fiber area is illuminated section by section instead of illuminating the same area all at once (Fig. 6), interference effects might be rather significant for the substructure within the diffraction maxima. To demonstrate the existence and the effect of such interference, an optical system was developed that allowed, by either a double slit or a beam-splitter/mirror combination (Fig. 1), the illumination of two areas within the fiber either one at a time or both together. For the overall geometry of the double beam arrangement, see Fig. 8 *e*. As shown in Fig. 8 *d*, the resulting diffraction maximum when both areas are illuminated simultaneously is not the sum of the two diffraction maxima observed when the two areas were illuminated one at a time (Fig. 8, *a* and *b*) and these two diffraction maxima were added by superposition of the two films (Fig. 8 *c*). Rather, additional "line splitting" is observed (Fig. 8 *d*). The separation of these "additional" lines is closely proportional to the

distance between the two illuminated fiber areas (Fig. 8 *f*).

DISCUSSION

Direct Correlation between Intensity Peaks in ω-Scans and Single Domains

Single skinned rabbit psoas fibers were shown to be very homogenous in sarcomeric structure (Brenner, 1983). This made possible the attempt to test directly the hypothesis that a single peak in the ω-scans represents the contribution of one single domain to the total intensity of the diffraction line under study, i.e., the hypothesis of a one to one correlation between intensity peaks and domains. The present data show that, in contrast to frog fibers, single skinned rabbit psoas fibers produce only a few distinct and narrow peaks in the ω-scans. Comparing ω-scans of left- and right-hand first-order diffraction lines, only pairs of peaks, matching in shape and amplitude were found, with rather constant separation between corresponding peaks. In no case were peaks observed of the type predicted for grating diffraction by the theory of Baskin et al. (1981 [see Fig. 7 and 8 of this reference]). These findings, together with the close correlation between predicted and observed incidence angle for the intensity peaks in the ω-scans, confirm that light diffraction in single skinned rabbit psoas fibers is dominated by Bragg diffraction (Rüdel and Zite-Ferenczy, 1979*a, b*); and, further, they suggest that each peak in the ω-scans represents the contribution of only one single domain.

However, to postulate a direct correlation between domains and peaks in ω-scans, one must consider the possibility that each of the distinct peaks might contain contributions from several domains. This, however, appears very unlikely. Estimating the diameter of domains from the FWHM of intensity peaks in such ω-scans that show only a single intensity peak, I found (Fig. 3, *a* and *b*, and Fig. 5 *b*) that the diameter of these domains is ~70–80% of the fiber diameter. The difference between domain diameter and fiber diameter either indicates that additional domains are present in the cross-section or reflects some broadening of the intensity peaks in the ω-scans due to some small variation in tilt angle and sarcomere length around their mean values even within a single domain. The latter suggestion appears not impossible since living systems very likely represent nonperfect crystals even on the domain level. A second domain making up for the difference between the calculated domain diameter and the fiber diameter in Fig. 3, *a* and *b*, could only have a diameter of, at most, 20–25 μm in the plane of the micrograph (Fig. 3 *a*). Such a domain would produce an intensity peak in the ω-scan with a FWHM of at least 5.3°, even if one assumed it was a perfect crystal. More than one additional domain making up for the difference would produce even wider peaks in the ω-scans. Thus, the narrow FWHM of the peaks that dominate the ω-scans of Fig. 3 *b* allows only for one large domain to cause this peak. Similar calculation also applies for the ω-scans on which the correlation in Fig. 5 *b* is based on. Possible additional, but necessarily much smaller domains, not accounted for by the dominating peaks in the ω-scans, could only be the source of much smaller and wider additional peaks or of the "background" around the main peaks. Thus, the data of Fig. 3, *a* and *b*, and Fig. 5 *b* indicate that it is almost impossible that more than one domain contributes to the dominating peaks in ω-scans. Two or more domains, located along the fiber, could, in principle, contribute to one narrow intensity peak in the ω-scan, only if their various combinations of sarcomere lengths and striation tilts are such that the Bragg condition is fulfilled at the same incidence angle. However, such a situation appears rather unlikely. Most likely, differences in the angle at which the Bragg condition is fulfilled will cause multiple peaks in the ω-scans or at least broadening of the peaks. However, as demonstrated in Fig. 5 *b* not much room is left for broadening, since otherwise the unresolved peaks of the contributing domains have to be narrower than the limit reached when the domain diameter equals the fiber diameter. In addition, the already narrow range of possible broadening is further restricted by any variation in sarcomere length and striation tilt within a domain. Therefore, evidence strongly suggests that each of the distinct intensity peaks within ω-scans represents the contribution of a single domain within the illuminated fiber region, as was originally postulated by Rüdel and Zite-Ferenczy (1979*a, b*).

The Origin of Substructural Lines within Diffraction Maxima

The attempted correlation of each substructural line with a single domain (Cleworth and Edman, 1972; Rüdel and Zite-Ferenczy, 1979*b*; Tameyasu et al., 1982; Leung, 1983; Zite-Ferenczy et al., 1984; Sundell et al., 1984, 1985) was shown to be inconsistent with several experimental results. First, substructural lines, observed in the diffraction line of a certain fiber area, are virtually absent when the same fiber area is illuminated segment by segment and all the diffraction maxima of these segments are summed photographically (Fig. 6). Of course, this experiment is only an approximation of the ideal case in which exactly one domain is illuminated at a time. Since the slit width can only be set to approximately the length of a domain, sometimes more than just a single domain might be illuminated. In addition, domains located side by side will be illuminated together. Still, the expected pattern of the substructural lines should be at least qualitatively similar to the pattern observed when the whole area is illuminated together. Second, when the length of the illuminated fiber segment is reduced, the observed increase in line separation and decrease in the number of substructural lines is in total disagreement with the prediction from

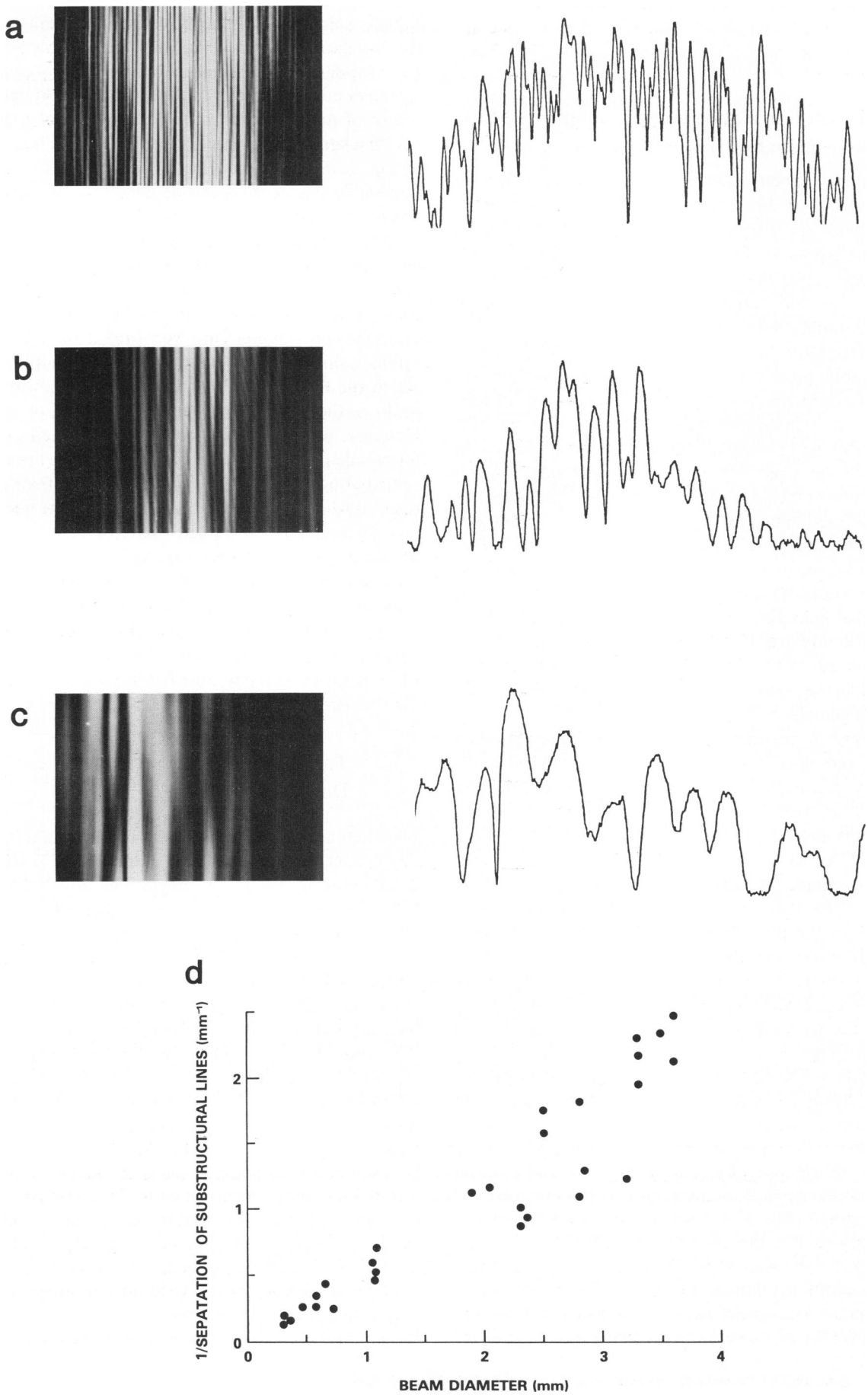
a
b
c
d
1/SEPATATION OF SUBSTRUCTURAL LINES (mm⁻¹)
0
1
2
0
1
2
3
4
BEAM DIAMETER (mm)

the hypothesis that each substructural line represents the diffraction line of a single domain. In this case, since all substructural lines have almost the same width (Fig. 7 *a*), the required length of all domains producing such narrow lines has to be approximately equal to the length of the illuminated area. Therefore, only the width of the substructural lines should increase when the beam diameter is reduced. Separation and number of the substructural lines, however, should remain unchanged.

An alternative hypothesis about the nature of the substructural lines is suggested by the results shown in Fig. 6. Since substructural lines are only observed when a fiber segment is illuminated simultaneously, interference between several domains that contribute to the diffraction pattern at the same time has to be considered. The existence and the strength of such interference has been demonstrated by the dual-beam or double-slit experiment. The observed "line splitting," with line width and separation inversely proportional to the separation between the two illuminated fiber areas, is exactly what one expects from diffraction theory when two objects, spaced by some distance, are illuminated at the same time by a light source with sufficient spatial coherence (see Fig. 2.5 in Squire, 1981).

Of course, to observe interference fringes, the diffraction maxima of the interfering domains have to overlap. From the dispersion in sarcomere length within a domain and the length of a typical domain, the expected width of the line-shaped diffraction maximum of a single domain can be calculated. The dispersion in sarcomere length can be estimated from the micrograph of Fig. 3 *a*, since the ω-scans of this fiber region (Fig. 3 *b*) are dominated by one peak that can only account for one large domain (see above). Because of this dispersion of sarcomere lengths within a domain the equilibrium positions of sarcomeres within a domain are not rigidly defined, but are only described by a probability distribution of nearest-neighbor positions, that is, by the probability distribution of sarcomere lengths. This, however, is characteristic of liquid-like disorder, i.e., "disorder of the second kind" (Guinier, 1963; Vainshtein, 1966). From calculations of the expected width of the diffraction maxima of single domains (Guinier 1963; Vainshtein, 1966), it follows that the FWHM of diffraction maxima of single domains corresponds to ~3% of the mean sarcomere length. In other words, a difference of ~3% in the mean sarcomere lengths of two domains will result in meridional displacement of the two corresponding diffraction maxima by one FWHM (that is, the overlap between the two diffraction maxima will be ~50%). Thus, it appears realistic to assume significant overlap between diffraction maxima of single domains, especially in the rather regular single skinned rabbit fibers in which variation in mean sarcomere length from domain to domain is well within 3%.

That all substructural lines, in fact, represent interference fringes is supported by several lines of evidence: First, intensity between substructural lines is low (see densitometer traces of Fig. 7), even when these lines are very closely spaced. Second, width and separation of the substructural lines is surprisingly regular (Fig. 7, *a–c*), much in contrast to expected variability when diffraction maxima of single domains with statistical variation in mean sarcomere length would superimpose without interference. Third, all substructural lines are affected by variation in beam diameter in the very same way, i.e., width and separation change inversly proportional to the beam diameter and their regular appearance remains unchanged. Therefore, most likely all the substructural lines within the diffraction maxima of single rabbit psoas fibers represent interference fringes due to interference between the various domains contributing to the diffraction maximum at that incidence angle.

This nature of substructural lines was recently discussed but rejected by Leung (1984). From the observed width and separation of the fine structure Leung calculated that the sarcomere length corresponding to adjacent fine structures differ by <1%. Leung concluded that differences in sarcomere length of the interfering fiber areas have to be <1% to produce sufficient overlap between the diffraction maxima of these areas. Such small variation in mean sarcomere length between various fiber areas was considered unrealistic. However, in his calculations Leung did not allow for any dispersion of sarcomere length within a domain that can cause significant broadening of the diffraction maxima of domains. An alternative hypothesis, also put forward by Leung (1984), attributing the substructure to wavefront distortion in the optically inhomogenous fiber, appears rather unrealistic, since only stepwise distortions of the wavefront were reported to introduce substructure in the calculated diffraction maxima. Thus, for regular substructures this hypothesis depends on the existence of regular stepwise optical inhomogeneities in the

FIGURE 7 Effect of beam diameter on width and separation of substructural lines. (*a–c*) Photographs of parts of the first-order diffraction maxima (*left*) with corresponding typical densitometer traces (*right*). Fiber-film distance, 1,700 mm. Same fiber for all examples. Beam diameters are: (*a*) 3.5, (*b*) 1.8, and (*c*) 0.5 mm. Widths of substructural lines are (*a*) 0.32 ± 0.01, (*b*) 0.62 ± 0.03, and (*c*) 1.54 ± 0.06 mm. Separations of substructural lines are (*a*) 0.42 ± 0.01, (*b*) 0.87 ± 0.06, and (*c*) 2.05 ± 0.25 mm. The widths of substructural lines was approximated by measuring the distance between two adjacent intensity minima in the densitometer traces. Note, the regular appearance of the substructural lines in any of the diffraction maxima. (*d*) Separation of substructural lines vs. beam diameter. Data of four experiments summarized. Note, since the total width of the diffraction maximum is unchanged, the total number of identifiable substructual lines is about proportional to the beam diameter. Fiber-film distance, 1,700 mm.

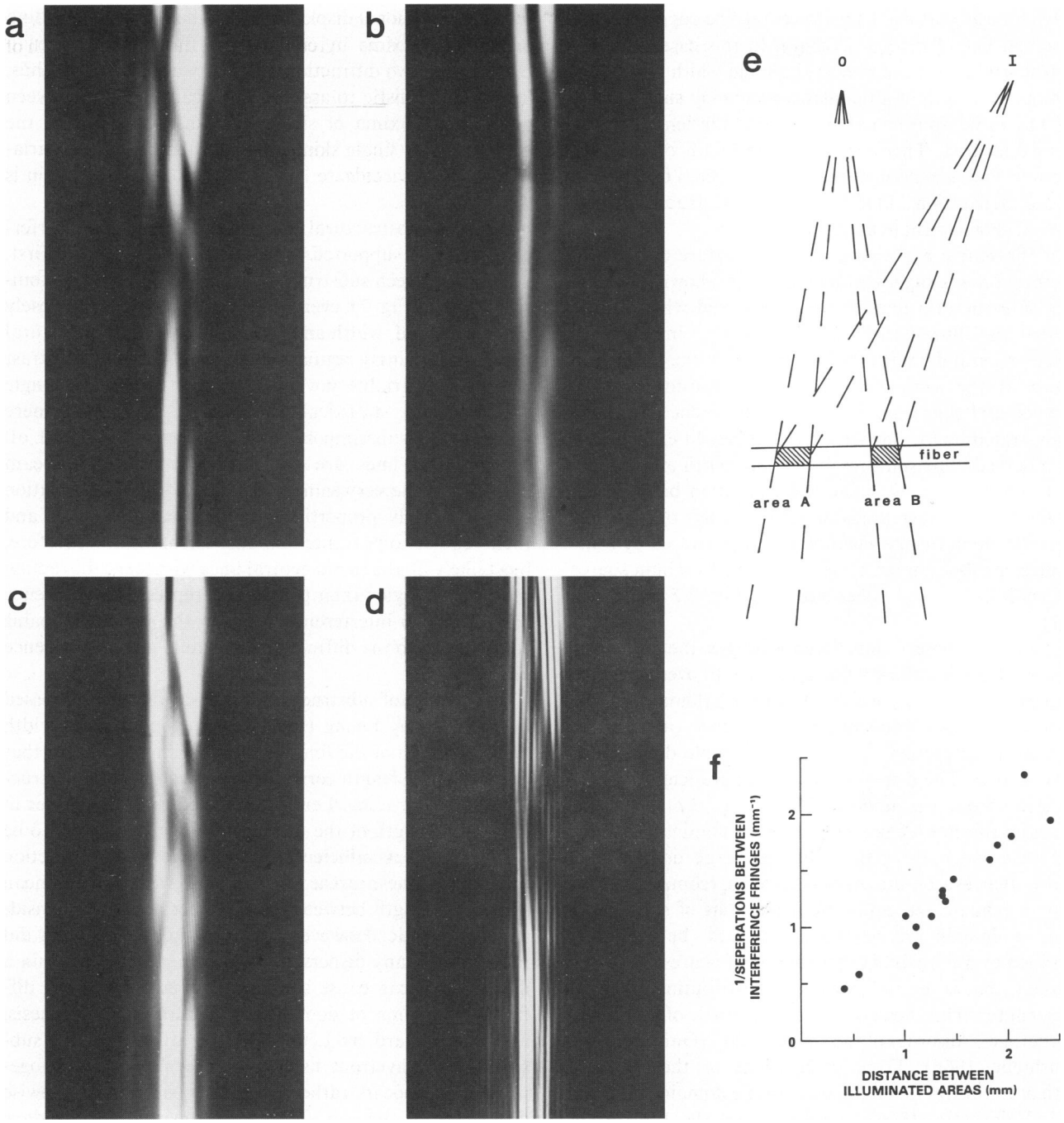

FIGURE 8 Double-beam experiment. Effect of simultaneous illumination of two fiber areas, *A* and *B*, within a fiber. (*a*) First-order diffraction maximum observed when only area *A* is illuminated. (*b*) First-order diffraction maximum observed when only area *B* is illuminated. (*c*) Sum of first-order diffraction maxima of *A* and *B*, obtained by superposition of the two films shown in *a* and *b*. (*d*) First-order diffraction maximum observed when *A* and *B* are illuminated simultaneously. Note, that here the "underlying" intensity distribution is similar to *c*, but there is also "line splitting" as the result of interference between *A* and *B*. (*e*) Schematic drawing on the optical arrangement. Note, the two beams are arranged such that their foci superimpose in the film plane. This is achieved by either the beam-splitter/mirror system (Fig. 1) or by placing a double slit in the path of an expanded beam focused onto the film plane. (*f*) Effect of center-center distance between the two illuminated areas on the width of the additional lines (interference fringes), observed when both areas were illuminated simultaneously (*d*).

fiber. Moreover, it appears unlikely that wavefront distortion can explain the results of Fig. 8 without reintroducing interference between the various fiber areas as the main cause of the substructural lines.

Therefore, the only explanation for the nature of the substructural lines that is consistent with all the experimental data is that these substructural lines in fact are interference fringes caused by interference between the different domains contributing to the diffraction maximum of a fiber.

Factors Affecting Intensity Distribution within Diffraction Maxima of Muscle Fibers

The envelope and substructure of the intensity of diffraction maxima produced by single muscle fibers can easily be explained on the basis of the sarcomeric domain organization with these domains acting as light-diffracting objects.

The intensity envelope (Fig. 6, *a* and *b* [note the conserved overall intensity distribution]) most likely reflects the superimposed diffraction maxima of the various contributing domains. First, the number of maxima in the intensity envelope (Fig. 6 *a*) agrees well with the number of domains expected to contribute to the diffraction maximum at the particular incidence angle at which the diffraction maximum is studied. This is the number of peaks in a series of ω-scans (Fig. 5 *a*) with significant intensity at this incidence angle. Second, the calculated width of the diffraction maximum, expected for a single domain (see above), agrees well with the observed width of the maxima in the intensity envelope recorded under conditions by which interference effects were minimized (Fig. 6 *a*).

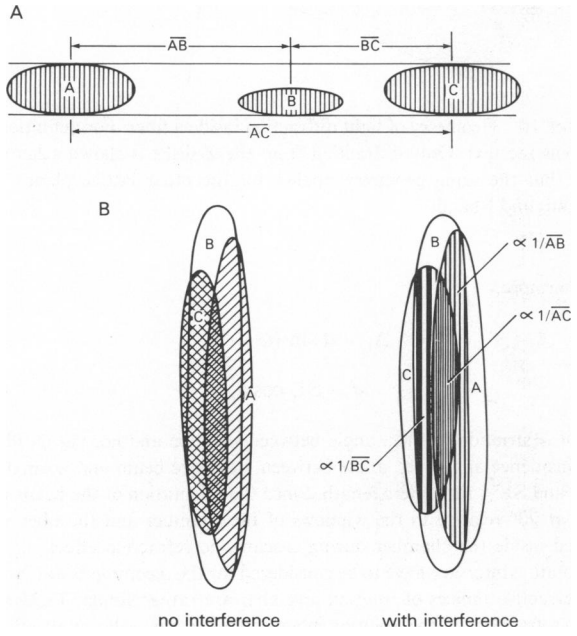

FIGURE 9 Schematic drawing of the effect of sarcomeric domain organization on first-order diffraction maxima. (*a*) Scheme of fiber with three major domains that contribute to the first-order diffraction maximum at a selected incidence angle. Domains not contributing at this incidence angle are located in the unassigned areas. $\overline{AB}$, $\overline{BC}$, and $\overline{AC}$ represent the center-to-center distance between the various domains. (*b*) Scheme of expected first-order diffraction maximum with (*right*) and without (*left*) interference between the domains. Sarcomere length and striation tilt of the three domains are assumed to be somewhat different, such that only partial overlap occurs between the diffraction lines of the three domains. Note, in rather regular fiber segments essentially all substructural lines are interference fringes and none is the equivalent of the diffraction maximum of a single domain. Nonoverlapping parts are only found in the faint periphery of the line-shaped diffraction maximum and do not represent diffraction maxima of single domains. When several diffraction maxima overlap, the fringe pattern with the highest spatial frequency will determine the width and separation of the substructural lines. Thus, separation and width are proportional to $1/\overline{AB}$ when *A* and *B* overlap, proportional to $1/\overline{BC}$ when *B* and *C* overlap, but proportional to $1/\overline{AC}$ when all three diffraction lines overlap (*center*).

This intensity envelope is modulated by interference if at the particular incidence angle several domains contribute to the diffraction maximum of the fiber and at least some overlap occurs between the diffraction maxima of these domains. The width of the substructural lines, equal to the distance between adjacent intensity minima, is determined by the fringe pattern with the highest spatial frequency, i.e., by those of the contributing domains with overlapping diffraction maxima that are separated furthest apart (Fig. 9). Not all the diffraction maxima of contributing domains might overlap at each point within the diffraction maximum (Fig. 9). Therefore, width and separation of substructural lines might vary somewhat in different areas of the diffraction maximum of a fiber. The magnitude of the intensity modulation by interference will depend on the relative intensities of the diffraction maxima of the interfering domains. The relative intensities will be determined by the intensities of the diffraction maxima of the interfering domains at the particular incidence angle, the detailed shape of these diffraction maxima, and the way these diffraction maxima overlap. This might explain at least some of the variation in the magnitude of the substructure (Fig. 7, *a–c*) and the large changes observed in the substructure when the incidence angle ω is changed (author's unpublished results).

As a way to explain the intensity distribution within diffraction maxima of single fibers, this idea is well supported by experiments in which the illuminating laser beam is moved along the fiber (Leung, 1984, Sundell et al., 1984, 1985; and author's unpublished results). While maxima in the intensity envelope (Fig. 6 *a*) persist as long as the corresponding domain is illuminated, i.e., for movements of the beam up to about one beam diameter, the detail of the substructure is changing almost continuously (see Fig. 6 of Leung, 1984; and author's unpublished results). In such experiments, in fact, appearance and disappearance of substructural lines of high intensity but of changing size and shape is followed. This is equivalent to following appearance and disappearance of maxima in the intensity envelope, i.e., following the contribution of one domain. The continuous changes in shape and size of the substructural lines indicate that the interference situation is changed already by very small translations of the beam.

Implications for Sarcomere Length Measurements by Laser Light Diffraction

The present results show that single skinned rabbit psoas fibers are organized in domains of somewhat different sarcomere length and tilt of striation. Within a 1-mm fiber segment of average homogeneity about eight different domains can be identified. Individual domains make strong

contributions to the diffraction maxima only when the incidence angle of the laser beam is such that the Bragg condition is met or almost met. The contribution of individual domains to the diffraction pattern at various incidence angles can be derived from the location and shape of their intensity peaks within ω-scans. Since different domains might vary significantly in their average sarcomere length, it is vital for highly accurate measurements of the sarcomere length by laser light diffraction to insure that the sarcomere length signal is always sampled from either one single domain or at least from the same group of domains throughout an experiment. Otherwise, when different domains become dominant during an experimental maneuver, apparent discontinuities in the sarcomere length signal might arise from just the variation in sarcomere length between various domains (Rüdel and Zite-Ferenczy, 1979*b*). The present data show that monitoring ω-scans of single fibers can be used to follow the sarcomeric domain organization to insure that the domain organization within a fiber does not change significantly during an experimental maneuver, or at least the relative contributions of the various domains remain unchanged. This approach was successfully used to measure sarcomere length in relaxed fibers (Brenner et al., 1982).

The present data also show that monitoring the position of a single substructural line cannot be used to directly measure the sarcomere length of a single domain as done by Tameyasu et al. (1982) and Leung (1983). In fact, the substructural lines, in essence a fringe pattern caused by the interference between various contributing domains, will put limits on the resolution of sarcomere length measurements by laser diffraction. Changes in the sarcomeric domain organization during experimental maneuvers can cause movement and changes of the fringe pattern, which in turn might produce changes in the diffraction signal, not reflecting real changes in sarcomere length.

APPENDIX

Calculation of the Incidence Angle ω Necessary to Observe a Maximum of Intensity in ω-Scans

Considering light diffraction in single fibers as Bragg diffraction from the lattice planes of the contractile proteins (Rüdel and Zite-Ferenczy, 1979*a*), a maximum of intensity in ω-scans will be observed at the incidence angle ω at which the Bragg condition is fulfilled, i.e., the difference in the total light path between successive lattice planes, Δ_1 plus Δ_2, (Fig. 10) is equal to the wave length of the light inside the fiber, λ_{fiber}, which is equal to λ_0/n_{fiber} (λ_0 = wave length of laser light in vacuum, n_{fiber} = refractive index of fiber)

$$\Delta_1 + \Delta_2 = \lambda_{fiber}. \tag{1}$$

Due to symmetry, $\Delta_1 = \Delta_2$. Therefore,

$$\lambda_{fiber} = 2_{\Delta_1}. \tag{2}$$

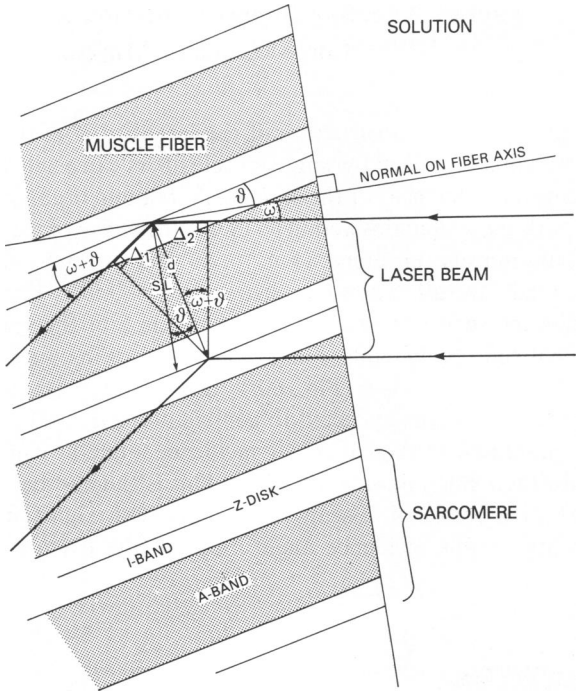

FIGURE 10 Geometry of light diffraction inside a fiber. For definition of symbols see text. Only diffraction from the Z-disks is shown schematically, but the same geometry applies for the other lattice planes like A-bands and I-bands.

Furthermore,

$$\Delta_1 = d \sin(\omega + \theta) \tag{3}$$

$$d = \mathrm{SL} \cos\theta, \tag{4}$$

with θ = striation tilt, i.e., angle between striation and normal on fiber, ω = incidence angle, i.e., angle between incidence beam and normal on fiber, and SL = sarcomere length. Since the orientation of the beam was fixed at 90° relative to the windows of the chamber and the fiber was rotated inside the chamber during ω-scans, no refraction effects at the air/solution interface have to be considered for the incoming beam. Since the refractive indices of solution and fiber are rather similar (1.35 and 1.37) refraction at the solution/fiber interface has only small effects (<2%) and is therefore ignored. From Eqs. 2, 3, and 4,

$$\lambda_{fiber} = 2\,\mathrm{SL} \cos\theta \sin(\omega + \theta) \tag{5}$$

or

$$\omega = \arcsin(\lambda_{fiber}/2\,\mathrm{SL} \cos\theta) - \theta. \tag{6}$$

Estimate of the Domain Diameter from the FWHM of Intensity Peaks in ω-scans

So far, only the incidence angle necessary to observe maxima of intensity in ω-scans was considered. This angle was derived from the Bragg equation. However, to estimate the intensity of diffraction maxima at various incidence angles around the Bragg angle, i.e., the intensities observed in ω-scans, the more general Ewald formalism (Fig. 11) has to be applied (Ewald, 1921; Bear and Bouldan 1950*a, b;* Fujime and Yoshino, 1978; Fujime, 1984; Zite-Ferenczy et al., 1984). According to

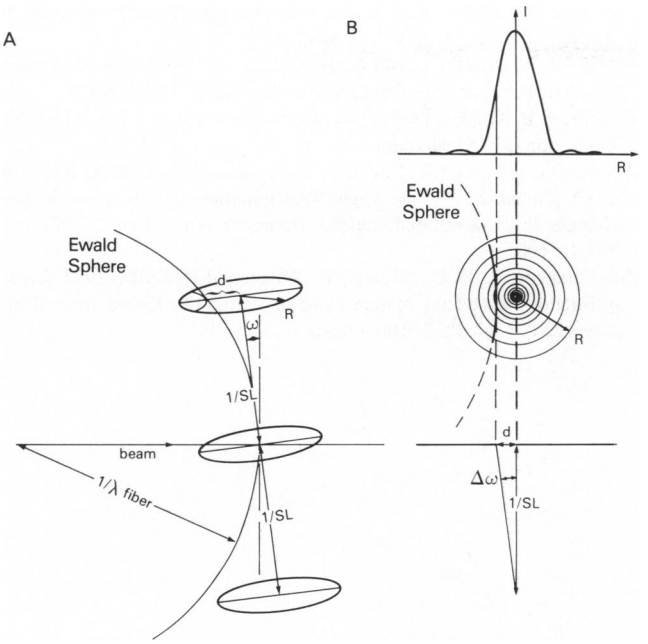

FIGURE 11 Light diffraction from a cylindrical diffracting unit with disks of high density, e.g., Z-disks, located along the axis of this cylinder with a periodicity of SL (sarcomere length). (*a*) Ewald construction for intensity of line-shaped diffraction maxima. The intersect between Ewald sphere and disk of diffractor in reciprocal space determines geometry and intensity of diffraction maximum. (*b*) *Top:* Intensity distribution on disks of diffractor in reciprocal space, $\propto (J_1(R)/R)^2$. J_1, first-order Bessel function; R, radius in reciprocal space. *Middle:* Intersection of Ewald sphere with disk in reciprocal space (viewed from top). The intensity distribution along the diffraction maximum is proportional to the intensity distribution on the disk along the intersection of the Ewald sphere. *Bottom:* Relation between d and $\Delta\omega$. $\Delta\omega$ is the difference between the actual incidence angle ω and ω_{max}, the incidence angle at which maximum intensity is observed in the diffraction line.

this formalism, the geometry and intensity of a diffraction line is determined by the intersect of the Ewald sphere with radius $1/\lambda_{fiber}$ and the representation of the light diffracting object in reciprocal space. In reciprocal space a muscle fiber with ideally aligned sarcomeres can be represented as a series of disks spaced by distance 1/SL along the reciprocal fiber axis (Fig. 11 *a*). The intensity distribution along the radius R of these disks (Fig. 11 *b*, top) is proportional to $(J_1(2\pi rR)/2\pi rR)^2$, with J_1 a first-order Bessel function, r the radius of diffracting disks in real space, and R the radius of disks in reciprocal space. The observed intensity in a diffraction line is proportional to the integrated intensity along the intersect between Ewald sphere and the corresponding disk in reciprocal space (Fig. 11 *b*). This integrated intensity is approximately proportional to the area of the section through the intensity profile where the Ewald sphere intersects, which is

$$\text{area} = \int_0^{I_{R-d}} 2\sqrt{R^2 - d^2}\, \mathrm{dI},$$

with d equaling the distance of intersect of Ewald sphere from the maximum of the intensity distribution, $I(R)$ (Fig. 11 *b*).

Numerical solution yields a function for the intensity in the diffraction maximum for different values of d, which is almost identical with the $(J_1(R)/R)^2$ function for $R < R_0$, the radius of the first minimum of this function. d is correlated with the incidence angle ω (see Fig. 11 *b*) by $\tan \Delta\omega = d$ SL, with $\Delta\omega$ being the difference between the incidence angle ω and the incidence angle ω_{max}, at which maximum intensity is observed in the diffraction line.

The calculated d to observe half maximum intensity in the diffraction line is about 0.44 R_0, with R_0 being equal to the position of the first minimum of the intensity distribution on the disk in reciprocal space. $2\pi rR$ for this minimum is 3.83, therefore, the radius r of the diffracting unit is $r = 3.83 \times 0.44/2\, d\pi$ or $r = 0.265$ SL/tan $\Delta\omega$. Since the difference between the two incidence angles at which half maximum intensity is observed (FWHM) equals $2\Delta\omega$, the diameter D of the diffracting unit (domain) is $D = 1.06$ SL/2 tan $\Delta\omega$.

The author is grateful to Dr. F. Zite-Ferenczy for many critical and stimulating discussions. He also would like to thank Dr. B. Trus for taking the densitometer traces and Dr. L. C. Yu for many suggestions and critical comments on the manuscript.

This work was supported by the Deutsche Forschungsgemeinschaft, grant Br 849/1-1.

Received for publication 18 April 1985 and in final form 31 July 1985.

REFERENCES

Baskin, R. J., R. L. Lieber, T. Oba, and Y. Yeh. 1981. Intensity of light diffraction from striated muscle as a function of incident angle. *Biophys. J.* 36:759–773.

Bear, R., and D. Bouldan. 1950*a*. Deficiencies in order of large size in fibrous systems. *Acta Crystallogr.* 3:230–235.

Bear, R., and D. Bouldan. 1950*b*. Diffraction of cylindrical bodies with periodic axial structure. *Acta Crystallogr.* 3:236–241.

Brenner, B. 1980. Effect of free sarcoplasmic Ca^{2+} concentration on maximum unloaded shortening velocity: measurements on single glycerinated rabbit psoas muscle fibers. *J. Muscle Res. Cell Motil.* 1:409–428.

Brenner, B. 1983. Technique for stabilizing the striation pattern in maximally calcium-activated skinned rabbit psoas fibers. *Biophys. J.* 41:99–102.

Brenner, B. 1985. Laser light diffraction in single skinned rabbit psoas fibers. The nature of the substructure within diffraction lines. *Biophys. J.* 47 (2, Pt. 2):383*a*. (Abstr.)

Brenner, B., M. Schoenberg, F. M. Chalovich, L. E. Greene, and E. Eisenberg. 1982. Evidence for cross-bridge attachment in relaxed muscle at low ionic strength. *Proc. Natl. Acad. Sci. USA.* 79:7288–7291.

Cleworth, D. R., and K. A. P. Edman. 1972. Changes in sarcomere length during isometric tension development in frog skeletal muscle. *J. Physiol. (Lond.).* 227:1–17.

Ewald, P. P. 1921. Das "reziproke Gitter" in der Strukturtheorie. *Z. f. Kristall.* 56:129–156.

Fujime, S., and S. Yoshino. 1978. Optical diffraction study of muscle fibers. I. A theoretical basis. *Biophys. Chem.* 8:305–315.

Fujime, S. 1984. An intensity expression of optical diffraction from striated muscle fibers. *J. Muscle Res. Cell Motil.* 5:577–587.

Guinier, A. 1963. X-ray Diffraction. Freeman & Co., San Francisco. 124.

Huxley, A. F. 1974. Muscular contraction. *J. Physiol. (Lond.).* 243:1–43.

Leung, A. F. 1983. Light diffractometry for determining the sarcomere length of striated muscle: an evaluation. *J. Muscle Res. Cell Motil.* 4:473–484.

Leung, A. F. 1984. Fine structures in the light diffraction pattern of striated muscle. *J. Muscle Res. Cell Motil.* 5:535–558.

Moss, R. L. 1979. Sarcomere length-tension relations of frog skinned muscle fibers during calcium activation at short length. *J. Physiol. (Lond.).* 292:177–192.

Rüdel, R., and F. Zite-Ferenczy. 1979*a*. Interpretation of light diffrac-

tion by cross-striated muscle as Bragg reflexion of light by the lattice of contractile proteins. *J. Physiol. (Lond.)*. 290:317–330.

Rüdel, R., and F. Zite-Ferenczy. 1979*b*. Do laser diffraction studies on striated muscle indicate stepwise sarcomere shortening? *Nature (Lond.)*. 278:573–579.

Sandow, A. 1936. Diffraction patterns of the frog sartorius and sarcomere behaviour under stretch. *J. Cell. Comp. Physiol.* 9:37–54.

Squire, F. M. 1981. The Structural Basis of Muscular Contraction. Plenum Publishing Corp., New York.

Sundell, C. L., L. D. Peachey, and Y. E. Goldman. 1984. Interpretation of laser diffraction patterns from single muscle fibers. *Biophys. J.* 45(2, Pt. 2):102*a*. (Abstr.)

Sundell, C. L., Y. E. Goldman, and L. D. Peachey. 1985. Microstructure in near-field and far-field laser diffraction patterns of muscle fibers. *Biophys. J.* 47(2, Pt. 2):383*a*. (Abstr.)

Tameyasu, T., N. Ishide, and G. H. Pollack. 1982. Discrete sarcomere length distribution in skeletal muscle. *Biophys. J.* 37:489–492.

Vainshtein, B. K. 1966. Diffraction of x-rays by chain molecules. Elsevier Publishing Co., Amsterdam.

Zite-Ferenczy, F., and R. Rüdel. 1978. A diffractometer using a lateral effect photodiode for the rapid determination of sarcomere length changes in cross-striated muscle. *Pfluegers Arch. Eur. J. Physiol.* 374:97–100.

Zite-Ferenczy, F., K. D. Häberle, W. Wilke, and R. Rüdel. 1984. Light diffraction of skeletal muscle explained with the Ewald formalism. *Biophys. J.* 45(2, Pt. 2):10*a*. (Abstr.)